Journal of Molecular Structure, 176 (1988) 253-277
Elsevier Science Publishers B.V., Amsterdam — Printed in The Netherlands

VIBRATIONAL SPECTRA, NORMAL VIBRATIONS AND ROTATIONAL ISOMERISM OF ETHYL ACETATE AND THREE DEUTERATED ANALOGUES

YOSHIYUKI MIDO* and HIDENORI SHIOMI

Department of Chemistry, Faculty of Science, Kobe University, Nada-ku, Kobe 657 (Japan)

HIROATSU MATSUURA

Department of Chemistry, Faculty of Science, Hiroshima University, Higashisenda-machi, Naka-ku, Hiroshima 730 (Japan)

MIGUEL ANGEL RASO, M. VICTORIA GARCIA and JESUS MORCILLO

Departamento de Estructura Atómico-Molecular y Espectroscopía, Facultad de Ciencias Químicas, Universidad Complutense, 28040 Madrid (Spain)

(Received 7 October 1987)

ABSTRACT

IR and Raman spectra of ethyl acetates, $CH_3COOC_2H_5$, $CD_3COOC_2H_5$, $CH_3COOC_2D_5$ and $CD_3COOC_2D_5$, in the liquid and crystalline states have been recorded in the 3500-200 cm^{-1} region. These spectra are analysed on the basis of spectral comparison both among themselves and with spectra of the trichloro analogues $CCl_3COOC_2H_5$ and $CCl_3COOC_2D_5$ previously studied. All the ethyl acetates in the crystalline state give two completely separated carbonyl stretching Raman bands, suggesting that two, or an even number of molecules, exist in the crystal unit. Liquid-state spectra exhibit many band pairs arising from the *trans-trans* and *trans-gauche* conformers around CX_3CO-O-CX_2CX_3 axes ($X=H$ and D) and the bands of the *trans-trans* conformer persist in the crystalline state. Normal coordinate calculations for the four species have been carried out on the two isomeric models using an MVIB program. The results explain wavenumber shifts on deuteration and the nature and separation of band pairs satisfactorily, and suggest that a large amount of vibrational coupling exists among skeletal stretching vibrations.

INTRODUCTION

Many vibrational studies on esters have focused on carbonyl stretching vibrations, characteristic νC=O frequencies for specific rotamers, solvent effect and the influence of temperature on νC=O band intensity [1, 2]. Such studies, although they have provided important information on the rotational isomerism of α-substituents, are less informative on that of the $-O(CH_2)_nCH_3$ group.

---

*To whom all correspondence should be addressed.

0022-2860/88/$03.50

Moreover, it has been pointed out that criteria based on position of bands in the νC=O region are insufficient in some cases [3, 4]. Thus, it is of importance to examine all fundamental bands and spectral changes in relation to change of physical state.

We have examined a series of haloacetates, concentrating on vibrational spectra, rotational isomers and band pairs, conformations of rotamers and polymorphism, as well as studies on the νC=O region [5–12] . To date, the IR spectra in the 3500–700 cm^{-1} region of ethyl acetate and its deuterates in the liquid state have been published and the bands observed in the 3500–1300 cm^{-1} region assigned by Nolin and Jones [13]. The IR and Raman spectra of ethyl acetate (not deuterates) in the liquid and crystalline states (1000–280 cm^{-1}) were studied by Ogawa [14]. However, the problems of rotational isomerism, explanations of Raman spectra and far IR spectra, etc. have not been discussed fully.

In this paper, a detailed study of the IR and Raman spectra of ethyl acetate and three deuterates, $CD_3COOC_2H_5$, $CH_3COOC_2D_5$, and $CD_3COOC_2D_5$ (E-NCA-d_0, -d_3, -d_5 and -d_8, respectively), in the liquid and crystalline states is presented together with the results of normal coordinate calculations for two rotamers with the *trans-trans* and *trans-gauche* conformations about the $CH_3CO–O–CH_2CH_3$ axes.

EXPERIMENTAL

E-NCA was prepared by reacting acetic acid and ethyl alcohol in benzene and the three deuterates by the same reaction using as starting materials the corresponding light and heavy acetic acids, and light and heavy ethyl alcohols. The samples synthesized were purified by repeated distillations. Each purified sample was checked by gas chromatography to have purity of above 96.5%. Each E-NCA was prepared independently twice and the spectra of the two were compared to check for the existence of impurity bands.

The IR and Raman spectra were recorded on Hitachi EPI 2G, Perkin-Elmer 580 and Nicolet 60-SX FT IR and SPEX Ramalog 5M (480 nm excitation of a Coherent Radiation CR-4 Ar^+ laser) spectrometers. Calibrated wavenumbers are believed to be accurate to within $\pm 2\ \mathrm{cm}^{-1}$, unless observed bands are very weak and/or broad.

The liquid-state spectra were recorded by a capillary method (between two CsI plates for IR and in a tube for Raman). The crystalline-state IR spectra were measured by a deposition method (slow spraying of a sample on a cooling CsI plate and annealing) using an RIIC VLT-2 cell. The crystalline-state Raman data were obtained from a sample, packed in an ampoule and indirectly cooled, in a conventional Raman cryostat, by the method described previously [8]. The Raman spectra of E-NCAs in the liquid and crystalline states are shown in Figs. 1–4, the crystalline-state IR spectra in Figs. 5 and 6, together

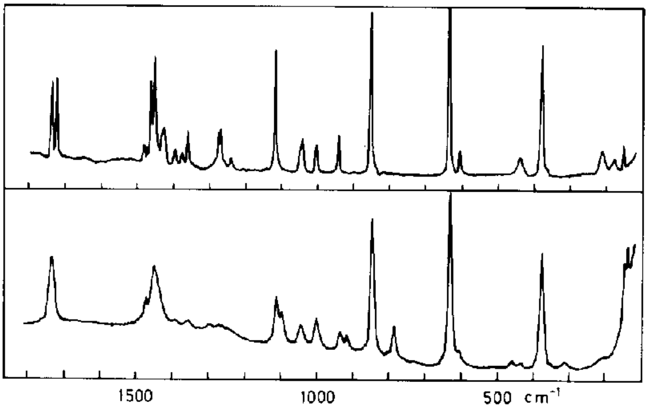

Fig. 1. Raman spectra of E-NCA-d_0 in the crystalline state at ca. 80 K (top) and liquid state at room temperature (bottom).

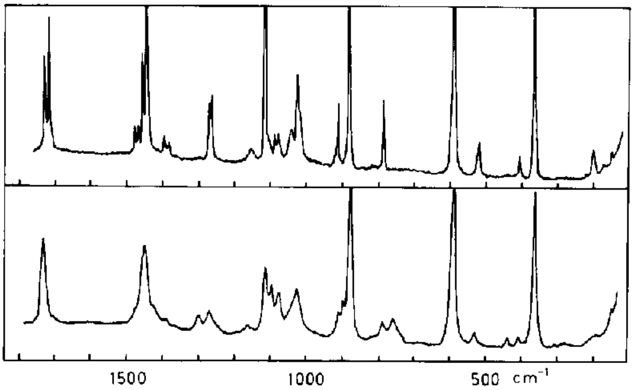

Fig. 2. Raman spectra of E-NCA-d_3 in the crystalline state at ca. 80 K (top) and liquid state at room temperature (bottom).

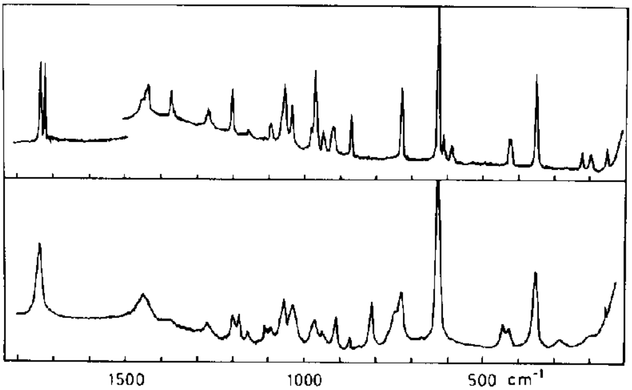

Fig. 3. Raman spectra of E-NCA-d_5 in the crystalline state at ca. 80 K (top) and liquid state at room temperature (bottom).

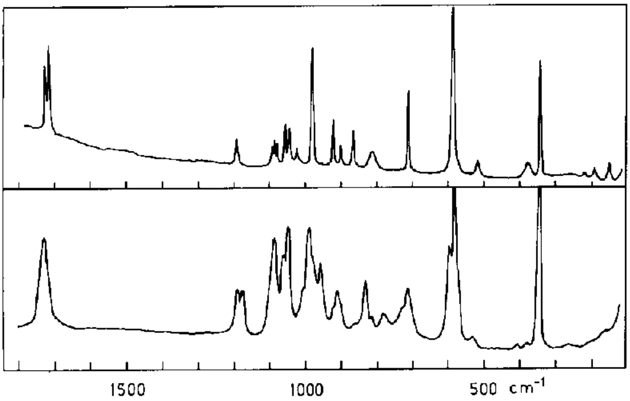

Fig. 4. Raman spectra of E-NCA-d$_8$ in the crystalline state at ca. 80 K (top) and liquid state at room temperature (bottom).

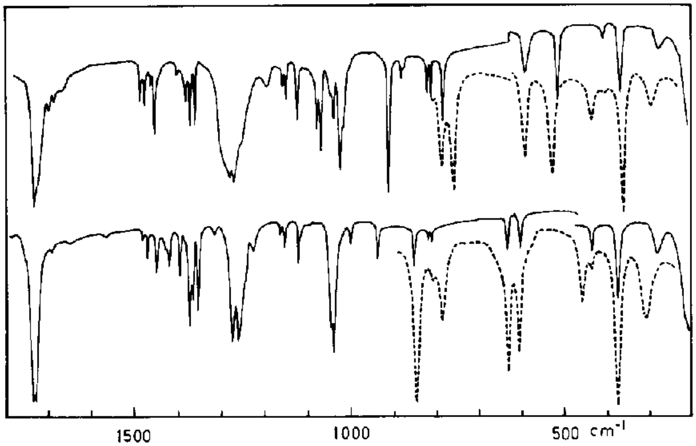

Fig. 5. IR spectra of E-NCA-$_0$ (bottom) and E-NCA-d$_3$ (top) in the crystalline state at ca. 130 K and liquid state at room temperature (800–200 cm^{-1}, dotted line).

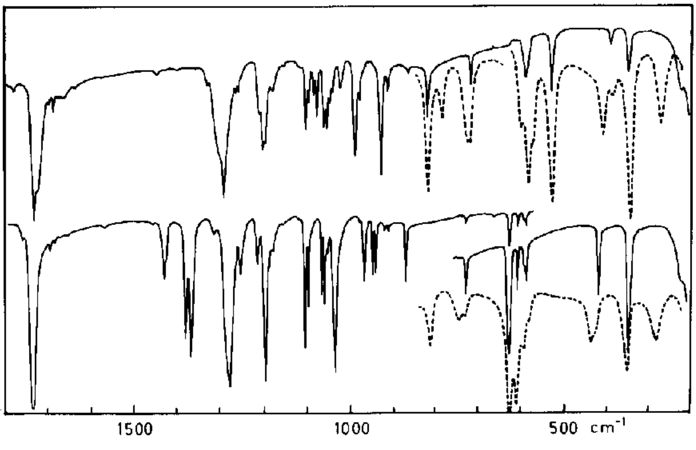

Fig. 6. IR spectra of E-NCA-d$_5$ (bottom) and E-NCA-d$_8$ (top) in the crystalline state at ca. 130 K and liquid state at room temperature (800–200 cm^{-1}, dotted line).

TABLE 1

Observed wavenumbers, in cm^{-1}, for $CH_3COOC'H_2CH_3$ and $CD_3COOC'H_2CH_3$ (E-NCA-d$_0$ and E-NCA-d$_3$)[a,b]

$CH_3COOC'H_2CH_3$ (E-NCA-d$_0$)				$CD_3COOC'H_2CH_3$ (E-NCA-d$_3$)				Assignment
Liquid		Crystal		Liquid		Crystal		
IR	Raman	IR	Raman	IR	Raman	IR	Raman	
		3022 vw	3030 w-m 3022 w-m					$\nu d CH_3O$
		2988 m	2989 m		2994 s		2991 s	$\nu d CH_3C$
2985 m	2985 mb	2979 m	2981 m	2985 m	2983 s	2980 m	2983 s	
2963 sh	2970 mb	2968 sh	2968 s			2974 sh	2971 s	$\nu a CH_2$
			2942 s			2948 sh	2945 m	$\nu d CH_3C$
2942 w	2940 w	2940 w	2936 s	2941 w	2941 vs	2940 w	2937 s	$\nu s CH_3O$
		2912 w	2916 w-m			2913 w	2914 m	$\nu s CH_3C$
2907 w	2904 w			2908 w	2907 m		2910 sh	
2877 w	2877 m	2876 w	2881 w-m	2878 w	2881 m	2879 w	2885 m 2881 m	$\nu s CH_2$
	2851 sh	2848 w				2850 vw		
				2266 w	2275 w	2269 vw	2273 s	$\nu d CD_3O$
				2238 vw	2244 w		2240 s	
				2168 vw	2176 m		2171 m	
				2123 vw	2126 s	2124 w 2116 w	2125 vs 2120 sh	$\nu s CD_3O$
1742 vs	1736 s	1739 vs	1738 s	1740 vs	1740 vs	1739 vs	1733 s	$\nu C=O$
		1732 vs	1724 s			1728 ssh	1720 s	
1480 m	1480 sh	1485 w	1483 w	1479 wsh		1485 w-m	1483 m	δCH_2
		1473 w-m	1473 w		1476 sh	1474 w-m	1472 m	
1466 m		1461 vw	1464 s	1467 m		1461 w	1461 vs	$\delta d CH_3C$
	1455 s	1451 m	1453 s		1455 s	1452 m	1451 vs	
1448 w				1447 m	1449 sh			(*G*)

TABLE 1 (continued)

$CH_3COOC'H_2CH_3$ (E-NCA-d_0)				$CD_3COOC'H_2CH_3$ (E-NCA-d_3)				Assignment	
Liquid		Crystal		Liquid		Crystal			
IR	Raman	IR	Raman	IR	Raman	IR	Raman		
1429 sh	1427 sh	1433 w 1425 vw	1425 m					$\delta d\mathrm{CH_3O}$	
		1399 w-m	1397 w			1401 w	1402 m	$\delta s\mathrm{CH_3C}$	
1393 w	1395 vw			1389 w-m	1392 sh		1389 m		
1374 m		1375 m-s	1376 w			1380 w-m		$\delta s\mathrm{CH_3O}$	
	1370 w	1368 m		1367 s		1370 m		$\delta w\mathrm{CH_2}$	
1361 w	1360 vw	1357 m	1361 m			1359 m			
1315 sh		1316 w				1325 sh			
1301 m	1300 vw			1298 sh	1302 w			$\delta t\mathrm{CH_2}$	(*G*)
1267 sh	1271 w	1275 s	1276 m		1270 w-m	1276 s	1273 m	$\delta t\mathrm{CH_2}$	(*T*)
		1262 s	1269 m			1268 s	1267 m	$\nu\mathrm{C{-}O}$	(*T*)
1241 vs	1245 w			1259 vs				$\nu\mathrm{C{-}O}$	(*G*)
1172 vw	1170 vw	1165 w						$\delta r\mathrm{CH_3C}$	(*G*)
1160 w		1165 w 1155 w-m				1153 w-m 1153 w-m	1159 wb	$\delta r\mathrm{CH_3C}$	(*T*)
		1122 w-m							
1113 m	1114 m	1117 sh	1118 s	1114 sh	1116 s	1124 m	1120 vs	$\delta r\mathrm{CH_3C}$	(*T*)
1098 m	1099 m			1095 ssh	1098 m			$\delta r\mathrm{CH_3C}$	(*G*)
				1077 s	1078 m	1083 m 1074 m-s	1082 w-m 1078 w-m	$\delta s\mathrm{CD_3O}$	
						1044 m	1048 m	$\delta d\mathrm{CD_3O}$	
1048 s	1048 w-m	1048 s 1042 s	1043 m	1027 s	1029 m	1031 s	1030 s	$\nu\mathrm{O{-}C'}/\nu\mathrm{C'C}$	
						1021 msh	1023 sh	$\delta d\mathrm{CD_3O}$	
1004 w	1002 w	1002 w	1004 m					$\delta r\mathrm{CH_3O}$	(*TG*)

938 m	939 w-m	940 w-m	942 m	915 m-s	911 w	916 vs	911 s	νC′-C	(T)
918 w	917 w-m			900 sh	897 w-m			νC′-C	(G)
847 w	846 s	852 w-m	851 vs	882 w-m	880 vs	885 w	885 vs	νC-C	(T G)
808 sh	814 vw	819 w 811 w		811 wsh	811 w	820 w-m 811 w-m	820 vw	δrCH$_2$	(T)/(TG)
786 w	786 w							δrCH$_2$	(G)
				789 m	790 m	789 m	790 m	δrCD$_3$O	(T)
				760 m	760 m			δrCD$_3$O	(G)
635 w	633 vs	634 w-m	635 vs	594 m	593 vs	595 w-m	595 vs	δC=O	(T G)
608 w	611 sh			531 m	532 w			πC=O	(G)
		602 w-m	604 w-m			521 m	523 m	πC=O	(T)
463 m	463 vw			441 vw	439 w			δCCO	(G)
441 w	439 vw	439 w	438 w-m	407 vw	409 w	410 w	410 w-m	δCCO	(T)
378 m	379 s	373 w-m	380 s	366 m	366 vs	363 m	370 vs	δOC′C	(T G)
313 wb	314 w			300 w	**			δCOC	(G)
254 vw^c	260 vw	284 w	**	?		282 w	280 wb	τCH$_3$C	
209 vw^c	203 wb	216 w?	211 w-m	?	200 vwb	203 w?	203 w-m	δCOC	(T)
160 vw^c	155 s	—	151 w-m	?	151 vw	—	148 w	τC-O	(T G)
136 vw^c	146 s	—			—	—			

---

[a] Spectral data for over- and combination tones in the 3500–3050, 2850–1800 and 1700–1500 cm^{-1} regions are omitted.

[b] Abbreviations used: s, strong; m, medium; w, weak; v, very; sh, shoulder; b, broad; ν, stretching; δ, deformation; δr, rocking; δw, wagging; δt, twisting; π, out-of-plane bending; τ, torsion; *s*, symmetric; *a*, asymmetric; *d*, degenerate; (*T*) and (*G*), the *trans-trans* and *trans-gauche* conformers of CH$_3$CO-O-CH$_2$CH$_3$ axes, respectively.

[c] Measured by using a polyethylene cell and a 12 μm beam splitter.

TABLE 2

Observed wavenumbers, in cm^{-1}, for $CH_3COOC'D_2CD_3$ and $CD_3COOC'D_2CD_3$ (E-NCA-d_5 and E-NCA-d_8)[a,b]

$CH_3COOC'D_2CD_3$ (E-NCA-d_5)				$CD_3COOC'D_2CD_3$ (E-NCA-d_8)				Assignment
Liquid		Crystal		Liquid		Crystal		
IR	Raman	IR	Raman	IR	Raman	IR	Raman	
		3028 vw	3028 m					νdCH_3O
2991 w	2986 wb	2990 w	2994 w-m					
	2947 vs	2948 sh	2955 s					νsCH_3O
2935 w		2940 w	2946 s					
					2270 w	2271 vw	2271 w-m	νdCD_3O
		2250 wsh 2243 wsh	2252 sh			2254 vw 2249 vw		νdCD_3O
2240 sh	2239 m	2235 wsh	2238 s	2245 m	2240 m	2240 vw	2248 s	νdCD_3C
2231 w		2223 w-m		2234 m		2236 w 2231 vw	2232 s	νaCD_2
		2210 vw	2206 vw			2210 vw	2211 w	νdCD_3C
2190 vw				2189 w	2188 w-m			
2153 w	2156 s	2160 w 2155 w	2166 w 2153 s	2154 w	2153 s	2158 w 2149 vw	2149 s	νsCD_2
2121 w		2122 w-m		2121 vw	2125 s	2123 vw	2121 m	νsCD_3O
	2115 m	2115 wsh	2116 w-m		2115 s	2115 w	**	νsCD_3C
2105 sh		2106 sh		2108 sh		2105 sh		
2074 w	2082 m	2073 w	2079 m	2077 w	2082 s	2075 w	2077 m	νsCD_3C
1740 vs	1740 s	1734 vs	1733 s	1738 vs	1732 vs	1736 vs	1729 s	$\nu C{=}O$
		1730 vs	1719 s			1728 s	1717 s	
	1452 mb	1455 vw	1454 w					δCH_3O
1436 w-m		1428 w-m	1428 m					
	1378 w	1377 m-s						δsCH_3O
1371 s		1365 s	1370 m					

		1273 s	1264 w			1290 vs		νC-O	*(T)*
1267 vs	1274 wh			1280 vs				νC-O	*(G)*
1194 s	1199 s	1195 s	1196 m	1196 s	1197 w-m	1199 s 1194 m-s	1197 w	νC'C/	*(T)*
1180 ssh	1184 m	(1176 w-m)		1177 w	1179 w	(1177 w-m)		δwCD$_2$	*(G)*
	1155 w	1154 vw	1153 w					νrCH$_3$O	
1102 s	1104 m	1103 s	**	1100 m		1103 m		δsCD$_3$C/δCD$_2$	
1089 msh	1092 m	1095 m	1093 m			1096 w	1097 w		
				1086 m-s	1091 m	1095 w-m 1078 m	1091 w 1080 w	δsCD$_3$O	
1063 s		1064 m 1058 m		1060 m-s	1061 w-m	1061 m			
	1055 s	1052 wsh			1053 m	1055 m	1057 m	δrCH$_3$O	
1050 msh		1049 wsh	1051 s	1050 m		1049 sh	1047 w	δdCD$_3$C	
						1023 w	1019 w	δdCD$_3$O	
1031 sh	1032 s	1033 s	1030 m	988 w-m	991 s-m	988 s	985 vs	νO-C'	
	974 s	978 vw	976 sh			978 w		δtCD$_2$	
964 w-m		966 m	966 s	959 w-m	960 m				
945 m	952 msh	946 m 938 m	943 w-m					δrCH$_3$O	
		920 w		918 w-m		923 s	923 m		
909 w-m	913 s	910 w	914 mb		913 w-m	908 w	903 w	νC'-C	
864 w-m	870 w	867 m	865 m	862 vw	865 vw	862 vw	863 m	νC-C	
809 w-m	813 s				839 w-m				
				816 w	820 vw	816 m	816 wb	δrCD$_3$O	*(T)*
				781 w	784 m			δrCD$_3$O	*(G)*
743 sh	743 sh			725 w	735 sh			δrCD$_3$C	*(G)*
727 sh	730 m	728 w	724 s	717 w	718 w	716 w-m	713 m-s	δrCD$_3$C	*(T)*
				599 w	599 m			-d$_3$ impurity?	

TABLE 2 (continued)

$CH_3COOC'D_2CD_3$ (E-NCA-d_5)				$CD_3COOC'D_2CD_3$ (E-NCA-d_8)				Assignment	
Liquid		Crystal		Liquid		Crystal			
IR	Raman	IR	Raman	IR	Raman	IR	Raman		
624 m	628 s	626 m	623 vs	583 w-m	583 vs	587 m	583 vs	δC=O	(TG)
611 m		608 w	608 m	527 w-m	530 w			πC=O	$(TG)/(G)$
						518 m	517 w	πC=O	(T)
590 w	**	588 w	589 w	583 w-m	583 vs	587 w-m	583 vs	δrCD$_2$	(T)
575 sh	581 s			572 w	576 sh			δrCD$_2$	(G)
436 w	439 w			408 m	408 w			δCCO	(G)
422 sh	423 w	420 w	419 m	385 sh	384 vw	382 w	382 w	δCCO	(T)
349 w	353 s	346 w-m	347 vs	344 m	346 s	341 w-m	344 vs	δOC′C	(TG)
279 w	284 wb			274 w	270 wb			δCOC	(G)
		223 w	220 w			221 w		τCD$_3$C	
—	200 vwb	—	197 w	185 vw^c		—	190 w	δCOC	(T)
—	155 w	—	150 w	148 w^c	152 vwb	—	148 w	τC–O	

^{a,b,c}See footnotes to Table 1.

with the liquid-state IR spectra (800–200 cm^{-1}). The observed wavenumbers are listed in Tables 1 and 2. The recorded liquid IR data are in agreement with the data of Nolin and Jones (3500–700 cm^{-1}) within experimental error, and the data for E-NCA-d_0 with those of Ogawa.

NORMAL COORDINATE TREATMENT

Normal coordinate calculations were carried out for ethyl acetate E-NCA-d_0, -d_3, -d_5 and -d_8. The *trans–trans* and *trans–gauche* molecular conformations were assumed for the bond axes $CH_3CO–O–CH_2CH_3$. The geometrical parameters were transferred from related molecules [15, 16]; bond lengths: $r(C_1–C_2)$ 1.518 Å, $r(C_2{=}O_3)$ 1.219 Å, $r(C_2–C_4)$ 1.360 Å, $r(O_4–C_5)$ 1.460 Å, $r(C_5–C_6)$ 1.539 Å and r(C–H) 1.100 Å; valence angles: $\angle$ $(C_1C_2O_4)$ 117.4°, $\angle$ $(C_1C_2O_3)$ 121.3°, $\angle$ $(O_4C_2O_3)$ 121.3°. $\angle$ $(C_2O_4C_5)$ 113.0°, $\angle$ $(O_4C_5C_6)$ 108.1°, $\angle$ (CCH) 110.4° and $\angle$ (OCH) 109.8°; dihedral angles: $\tau(C_1–C_2–O_4–C_5)$ 180° *trans* and $\tau(C_2–O_4–C_5–C_6)$ 180° *trans* and 60° *gauche.*

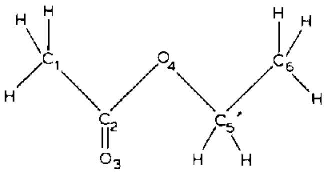

trans–trans conformer

The force field employed is the group coordinate force field [17], in which the force constants are expressed in terms of the group symmetry coordinates of the individual atomic groups constituting the molecule. The definition of these coordinates is in agreement with the IUPAC recommendation [18], full details of which are found elsewhere [17]. Most of the force constants for the ethyl acetate molecule were taken from the well-established force field for alkanes and alkyl ethers [16], which was supplemented by making allowance for the force field determined previously for alkyl ketones and alkyl esters [14].

Calculations were carried out with an MVIB computer program [17], developed for treating normal vibrations of chain molecules. Calculated frequencies and potential-energy distributions (PED) are given in Tables 3–6. In these calculations, we have adjusted ten significant force constants so that the agreement between observed and calculated frequencies has been much improved. We do not show the 86 force constants used for the sake of brevity; a tabulation of these is available from one of the authors (H.M.).

RESULTS AND DISCUSSION

Vibrational spectra of E-NCAs

The four E-NCAs in the crystalline state give two strong νC=O bands near 1740 cm^{-1}. They are much further apart in the Raman than in the IR spec-

TABLE 3

Observed (ν_{obs}) and calculated wavenumbers (ν_{calc}), in cm^{-1}, and potential energy distribution (PED) for the *trans-trans* (T) and *trans-gauche* (G) conformers of $\mathrm{CH_3CO{-}O{-}C'H_2CH_3}$ (E-NCA-d$_0$)

ν_{obs}	T conformer		G conformer	
	ν_{calc}	PED (%)^{a,b}	ν_{calc}	PED (%)^{a,b}
1739^{c}	1741 a'	$\nu\mathrm{C{=}O}\ (119)$	1741	$\nu\mathrm{C{=}O}\ (119)$
1480	1483 a'	$\delta\mathrm{CH_2}(88)$	1480	$\delta\mathrm{CH_2}(88)$
1466	1458 a'	$\delta d\mathrm{CH_3C}(77)\ \delta r\mathrm{CH_3C}(11)$	1458	$\delta d\mathrm{CH_3C}(76)\ \delta r\mathrm{CH_3C}(11)\ \delta\mathrm{CH_2}(10)$
1455	1452 a''	$\delta d\mathrm{CH_3C}(79)\ \delta r\mathrm{CH_3C}(15)$	1453	$\delta d\mathrm{CH_3C}(77)\ \delta r\mathrm{CH_3C}(15)$
1448	1448 a''	$\delta d\mathrm{CH_3O}(94)$	1448	$\delta d\mathrm{CH_3O}(94)$
1429	1444 a'	$\delta d\mathrm{CH_3O}(93)$	1444	$\delta d\mathrm{CH_3O}(93)$
1393	1391 a'	$\delta w\mathrm{CH_2}(67)\ \delta s\mathrm{CH_3C}(20)\ \nu\mathrm{C'C}(15)$	1390	$\delta w\mathrm{CH_2}(67)\ \delta s\mathrm{CH_3O}(14)$
1374	1375 a'	$\delta s\mathrm{CH_3O}(68)\ \delta w\mathrm{CH_2}(14)\ \delta s\mathrm{CH_3C}(13)$	1375	$\delta s\mathrm{CH_3C}(73)\ \delta s\mathrm{CH_3O}(20)\ \nu\mathrm{C'C}(11)$
1370	1370 a'	$\delta s\mathrm{CH_3C}(61)\ \delta s\mathrm{CH_3O}(24)$	1368	$\delta s\mathrm{CH_3O}(61)\ \delta w\mathrm{CH_2}(20)\ \delta s\mathrm{CH_3C}(19)$
1301			1304	$\delta t\mathrm{CH_2}(67)\ \delta r\mathrm{CH_2}(10)$
1275^{d}	1278 a''	$\delta t\mathrm{CH_2}(81)\quad [\delta s\mathrm{CH_3O}(13)$		
1262^{d}	1265 a'	$\nu\mathrm{CC}(48)\ \nu\mathrm{CO}(46)\ \delta\mathrm{C{=}O}(28)$		$[\delta s\mathrm{CH_3C}(10)$
1241			1256	$\nu\mathrm{CC}(48)\ \nu\mathrm{CO}(36)\ \delta\mathrm{C{=}O}(28)$
1160	1163 a''	$\delta r\mathrm{CH_3C}(38)\ \delta r\mathrm{CH_2}(30)\ \delta t\mathrm{CH_2}(13)$	1167	$\delta r\mathrm{CH_3C}(35)\ \delta r\mathrm{CH_2}(27)\ \delta t\mathrm{CH_2}(22)$
		$\delta d\mathrm{CH_3C}(12)$		$\delta d\mathrm{CH_3C}(11)$
1114	1125 a'	$\delta r\mathrm{CH_3C}(42)\ \nu\mathrm{C'C}(16)\ \delta\mathrm{OC'C}(14)$		$[\delta\mathrm{OC'C}(11)$
1099			1106	$\delta r\mathrm{CH_3C}(50)\ \nu\mathrm{C'C}(15)\ \delta d\mathrm{CH_3C}(11)$
1048	1049 a'	$\nu\mathrm{C'C}(38)\ \nu\mathrm{OC'}(32)\ \delta r\mathrm{CH_3O}(11)$	1048	$\delta r\mathrm{CH_3O}(55)\ \pi\mathrm{C{=}O}(17)$
1042^{d}	1044 a''	$\delta r\mathrm{CH_3O}(63)\ \pi\mathrm{C{=}O}(20)$	1037	$\nu\mathrm{C'C}(41)\ \delta r\mathrm{CH_3O}(19)\ \nu\mathrm{OC'}(16)$
1004	1008 a'	$\delta r\mathrm{CH_3O}(49)\ \delta\mathrm{CCO}(11)\ \delta r\mathrm{CH_3C}(10)$	998	$\delta r\mathrm{CH_3O}(36)\ \nu\mathrm{C'C}(25)\ \nu\mathrm{CC}(12)$
938	939 a'	$\nu\mathrm{OC'}(30)\ \nu\mathrm{CC}(32)\ \nu\mathrm{C'C}(16)$		

918			911	νCO(40) νCC(19) νOC′(10)
846	839 a'	νOC′(55) δrCH$_3$C(22) δwCH$_2$(17)	849	νOC′(43) δrCH$_3$C(14) δCOC(12) [δrCH$_2$(11)
814	815 a''	δrCH$_2$(60) δrCH$_3$C(48) [δCOC(15)		
786			790	δrCH$_2$(45) δrCH$_3$C(29) νCO(16)
633	627 a'	δC=O(51) νCC(21) νOC′(10)	633	δC=O(42) νCC(19) νOC′(12)
608	609 a''	πC=O(78) δrCH$_3$O(32)	616	πC=O(71) δrCH$_3$O(30)
463			463	δCCO(54) δOC′C(31) δC=O(23) [δCOC(18)
441	441 a'	δCCO(107) νC=O(19) δOC′C(18) δrCH$_3$O(17)		
378	385 a'	δOC′C(42) δCOC(17) δC=O(15)	385	δOC′C(51) δCCO(46)
314			314	δCOC(34) τCH$_3$O(24) δCCO(22)
254	249 a''	τCH$_3$C(91)	211	τCH$_3$C(92)
209	209 a'	δCOC(47) δOC′C(35) δCCO(20)		
	206 a''	τCH$_3$O(96)	204	τCH$_3$O(92)

Calculated wavenumbers higher than 2000 cm^{-1}; 2988 2985 2968 2962 2958 2941 2881 2864.

[a] See footnote [b] to Table 1 for abbreviations. [b] Main contributions; for bands below 200 cm^{-1} the PEDs are not exhibited because of unknown τC–O and τO–C′ force field. [c] Average value of IR and Raman wavenumbers. Liquid data are adopted, as a general rule. [d] Observed wavenumber in the crystal.

TABLE 4

Observed (ν_{obs}) and calculated wavenumbers (ν_{calc}), in cm^{-1}, and potential energy distribution (PED) for the *trans*-*trans* (*T*) and *trans*-*gauche* (*G*) conformers of CD_3CO-O-C$'H_2CH_3$ (E-NCA-d_3)

ν_{obs}	*T* conformer		*G* conformer	
	ν_{calc}	PED (%)^{a,b}	ν_{calc}	PED (%)^{a,b}
1740	1736 *a'*	$\nu C{=}O(121)$	1736	$\nu C{=}O(121)$
1479	1482 *a'*	$\delta CH_2(88)$	1479	$\delta CH_2(88)$
1467	1458 *a'*	$\delta dCH_3C(77)$ $\delta rCH_3C(11)$	1458	$\delta dCH_3C(75)$ $\delta rCH_3C(11)$ $\delta CH_2(10)$
1455	1452 *a''*	$\delta dCH_3C(79)$ $\delta rCH_3C(15)$	1453	$\delta dCH_3C(77)$ $\delta rCH_3C(15)$
1389	1390 *a'*	$\delta wCH_2(71)$ $\delta sCH_3C(19)$ $\nu C'C(15)$	1387	$\delta wCH_2(83)$
1367	1371 *a'*	$\delta sCH_3C(75)$ $\delta wCH_2(19)$	1373	$\delta sCH_3C(89)$
1302			1305	$\delta tCH_2(66)$
1276^{a}	1278 *a''*	$\delta tCH_2(81)$		
1268^{d}	1265 *a'*	$\nu CO(56)$ $\nu CC(40)$ $\delta C{=}O(31)$		[$\delta wCH_2(10)$
1259			1253	$\nu CO(42)$ $\nu CC(41)$ $\delta C{=}O(30)$
1162^{d}	1163 *a''*	$\delta rCH_3C(38)$ $\delta rCH_2(30)$ $\delta tCH_2(13)$ $\delta dCH_3C(12)$	1167	$\delta rCH_3C(35)$ $\delta rCH_2(27)$ $\delta tCH_2(22)$ $\delta dCH_3C(11)$
1116	1126 *a'*	$\delta rCH_3C(40)$ $\nu CC'(16)$ $\delta OC'C(14)$		
1098			1104	$\delta rCH_3C(52)$ $\nu CC'(13)$ $\delta dCH_3C(11)$
1077	1067 *a'*	$\delta sCD_3O(81)$ $\nu CC(25)$	1066	$\delta sCD_3O(84)$ $\nu CC(20)$ [$\delta OC'C(11)$

1048^d	1048 a'	$\delta d\mathrm{CD_3O}$(61) $\nu\mathrm{C'C}$(14) $\nu\mathrm{OC'}$(12)	1044	$\delta d\mathrm{CD_3O}$(90)
1048^d	1042 a''	$\delta d\mathrm{CD_3O}$(97)	1042	$\delta d\mathrm{CD_3O}$(97)
1027	1037 a'	$\nu\mathrm{C'C}$(34) $\delta d\mathrm{CD_3O}$(33) $\nu\mathrm{OC'}$(17)	1024	$\nu\mathrm{C'C}$(66) $\nu\mathrm{OC'}$(24)
915	914 a''	$\delta r\mathrm{CD_3O}$(40) $\pi\mathrm{C{=}O}$(41)	913	$\delta r\mathrm{CD_3O}$(40) $\pi\mathrm{C{=}O}$(41)
915	910 a'	$\nu\mathrm{OC'}$(20) $\nu\mathrm{CO}$(16) $\nu\mathrm{C'C}$(12) $\nu\mathrm{CC}$(12)		$\nu\mathrm{CO}$(12)
897			887	$\nu\mathrm{OC'}$(35) $\delta r\mathrm{CH_3C}$(16) $\delta w\mathrm{CH_2}$(12)
880	886 a'	$\delta\mathrm{CCO}$(30) $\nu\mathrm{OC'}$(18) $\nu\mathrm{CO}$(17)	889	$\delta\mathrm{CCO}$(25) $\nu\mathrm{CO}$(23) $\delta\mathrm{COC}$(12)
		$\delta r\mathrm{CD_3O}$(15)		[$\delta s\mathrm{CD_3O}$(11)
811	812 a''	$\delta r\mathrm{CH_2}$(60) $\delta r\mathrm{CH_3C}$(47)	813	$\delta r\mathrm{CH_2}$(31) $\delta r\mathrm{CH_3C}$(25) $\delta r\mathrm{CD_3O}$(17)
790	791 a'	$\delta r\mathrm{CD_3O}$(34) $\nu\mathrm{OC'}$(27)		[$\nu\mathrm{OC'}$(14)
760			769	$\delta r\mathrm{CD_3O}$(20) $\delta r\mathrm{CH_2}$(22) $\nu\mathrm{CO}$(16)
593	573 a'	$\delta\mathrm{C{=}O}$(38) $\nu\mathrm{CC}$(20) $\nu\mathrm{OC'}$(12)	592	$\delta\mathrm{C{=}O}$(29) $\nu\mathrm{CC}$(21) $\nu\mathrm{OC'}$(14)
531		[$\delta r\mathrm{CD_3O}$(12)	532	$\pi\mathrm{C{=}O}$(48) $\delta r\mathrm{CD_3O}$(53)
523^d	522 a''	$\pi\mathrm{C{=}O}$(55) $\delta r\mathrm{CD_3O}$(56)		
439			433	$\delta\mathrm{OC'C}$(46) $\delta\mathrm{C{=}O}$(25) $\delta\mathrm{COC}$(18)
409	400 a'	$\delta\mathrm{CCO}$(66) $\delta\mathrm{OC'C}$(48) $\delta r\mathrm{CD_3O}$(19)		[$\delta\mathrm{CCO}$(17)
		$\nu\mathrm{CO}$(14) [$\delta\mathrm{OC'C}$(12)		
366	377 a'	$\delta\mathrm{COC}$(28) $\delta\mathrm{C{=}O}$(23) $\delta\mathrm{CCO}$(22)	362	$\delta\mathrm{CCO}$(50) $\delta\mathrm{OC'C}$(31) $\delta r\mathrm{CD_3O}$(15)
300			306	$\delta\mathrm{CCO}$(41) $\delta\mathrm{COC}$(25) $\tau\mathrm{CH_3C}$(24)
	249 a''	$\tau\mathrm{CH_3C}$(93)		
200	201 a'	$\delta\mathrm{COC}$(43) $\delta\mathrm{OC'C}$(33) $\delta\mathrm{CCO}$(27)	209	$\tau\mathrm{CH_3C}$(70) $\delta\mathrm{COC}$(16)

Calculated wavenumbers higher than 2000 cm^{-1}; 2968 2962 2958 2881 2864 2235 2226 2122.

[a] See footnote [b] to Table 1 for abbreviations. [b,c,d] See footnotes to Table 3.

TABLE 5

Observed (ν_{obs}) and calculated wavenumbers (ν_{calc}), in cm^{-1}, and potential energy distribution (PED) for the *trans–trans* (*T*) and *trans-gauche* (*G*) conformers of CH$_3$CO-O-C′D$_2$CD$_3$ (E-NCA-d$_5$)

ν_{obs}	*T* conformer		*G* conformer	
	ν_{calc}	PED (%)^{a,b}	ν_{calc}	PED (%)^{a,b}
1740	1741 *a*′	νC=O(119)	1741	νC=O(119)
1452	1448 *a*″	δdCH$_3$O(94)	1448	δdCH$_3$O(94)
1436	1444 *a*′	δdCH$_3$O(93)	1444	δdCH$_3$O(93)
1371	1374 *a*′	δsCH$_3$O(93)	1374	δsCH$_3$O(93)
1273^d	1277 *a*′	νCC(45) νCO(37) δC=O(26) δsCH$_3$O(13)		
1267			1272	νCC(48) νCO(45) δC=O(28) [δsCH$_3$O(13
1197^c	1198 *a*′	νC′C(54) δwCD$_2$(30) δsCD$_3$C(12) [νCO(12)		
1182^c			1174	νC′C(64) δwCD$_2$(26) δsCH$_3$C(26)
1102	1100 *a*′	δsCD$_3$C(43) δCD$_2$(33)	1090	δCD$_2$(54) δsCD$_3$C(25)
1063	1060 *a*′	δdCD$_3$C(31) δwCD$_2$(22) δCD$_2$(18) δsCD$_3$C(13)	1071	δdCD$_3$C(17) δrCD$_2$(15) δtCD$_2$(13) δrCH$_3$O(13)
1055	1050 *a*″	δrCH$_3$O(40) δdCD$_3$C(19) πC=O(14)	1053	δdCD$_3$C(26) δwCD$_2$(25) δrCH$_3$O(15)
1050	1041 *a*′	δCD$_2$(35) δdCD$_3$C(27) δrCH$_3$O(10)	1048	δdCD$_3$C(31) δrCH$_3$O(15) δCD$_2$(13)
	1039 *a*″	δdCD$_3$C(53) δrCH$_3$O(21)	1039	δrCH$_3$O(73) δwCD$_2$(16)
1032	1025 *a*′	δrCH$_3$O(35) δdCD$_3$C(29) νOC′(16) δCCO(12)	1024	δdCD$_3$C(44) δrCH$_3$O(21) δCCO(10)
			1013	δdCD$_3$C(52) νOC′(11) δwCD$_2$(10)
974	965 *a*′	δrCD$_2$(22) νCO(16) δwCD$_2$(15) [δOC′C(14)		
964	962 *a*″	δrCD$_2$(36) δdCD$_3$C(23) δrCD$_3$C(15)		
945	942 *a*′	νOC′(33) νCC(33) νCO(10)	953	νOC′(31) νCC(18) δrCH$_3$O(13) [δrCD$_3$C(10)
913	902 *a*″	δtCD$_2$(81) δrCD$_3$C(18)	914	δtCD$_2$(46) δrCD$_3$C(28) δrCD$_2$(11)

			888	νC′C(20) δrCD$_3$C(15) δsCD$_3$C(15)
864	852 a'	νCC(25) δsCD$_3$C(23) νCO(15)		
813			812	νCO(40) δtCD$_2$(27)
743			739	δrCD$_3$C(28) δwCD$_2$(17) νOC′(13) [νCC′(13)
730	722 a'	δrCD$_3$C(46) δwCD$_2$(23) νOC′(15)		
624	618 a'	δC=O(53) νCC(18) δrCH$_3$O(10) δrCD$_3$O(12)	627	δC=O(30) δrCD$_3$C(16) νCC(14) νOC′(13)
611	625 a''	πC=O(45) δrCD$_3$C(22) δrCH$_3$O(20) δrCD$_2$(17) [δrCH$_3$O(12)	613	πC=O(75) δrCH$_3$O(31)
590	584 a''	δrCD$_2$(38) πC=O(33) δrCD$_3$C(31)		
581			586	δrCD$_2$(44) δrCD$_3$C(36) δC=O(20)
438[c]			441	δCCO(75) δCOC(17) δC=O(17) [δOC′C(16)
423	428 a'	δCCO(107) δC=O(19) δrCH$_3$O(16) [νOC′(13)		
353	351 a'	δOC′C(42) δCOC(18) δC=O(11)	358	δOC′C(59) δCCO(32)
279			276	δCOC(42) δCCO(15) τCD$_3$C(15)
	209 a''	τCH$_3$O(88)	204	τCH$_3$O(97)
200	194 a'	δCOC(45) δOC′C(41) δCCO(17)		
	186 a''	τCD$_3$C(79) τCH$_3$O(11)		

Calculated wavenumbers higher than 2000 cm^{-1}; 2988 2985 2941 2224 2212 2200 2103 2078.

[a] See footnote [b] to Table 1 for abbreviations. [b,c,d] See footnotes to Table 3.

TABLE 6

Observed (ν_{obs}) and calculated wavenumbers (ν_{calc}), in cm^{-1}, and potential energy distribution (PED) for the *trans–trans* (*T*) and *trans–gauche* (*G*) conformers of CD$_3$CO-O-C′D$_2$CD$_3$ (E-NCA-d$_8$)

ν_{obs}	*T* conformer		*G* conformer	
	ν_{calc}	PED (%)^{a,b}	ν_{calc}	PED (%)^{a,b}
1735^c	1736 *a*′	νC=O(121)	1735	νC=O(121)
1290^d	1277 *a*′	νCO(45) νCC(38) δC=O(29)		
1280			1272	νCO(55) νCC(40) δC=O(31)
1196	1198 *a*′	νC′C(53) δwCD$_2$(30) νCO(14)		
1178^c		[δsCD$_3$C(12)	1174	νC′C(66) δwCD$_2$(26) δsCH$_3$C(26)
1100	1101 *a*′	δsCD$_3$C(43) δCD$_2$(28)	1091	δCD$_2$(38) δsCD$_3$C(21)
1086	1072 *a*′	δsCD$_3$O(56) δCD$_2$(22) νCC(20)	1084	δsCD$_3$O(30) δCD$_2$(23) νCC(13)
1060	1056 *a*′	δdCD$_3$C(28) δsCD$_3$O(17) δwCD$_2$(15)	1054	δsCD$_3$O(27) δdCD$_3$C(19) δdCD$_3$O(18)
1053	1043 *a*′	δdCD$_3$O(77) δdCD$_3$C(13) [δdCD$_3$O(12)	1051	δdCD$_3$C(46) δwCD$_2$(18) δrCD$_3$C(12)
	1043 *a*″	δdCD$_3$C(53) δdCD$_3$O(22) δrCD$_3$C(12)	1044	δdCD$_3$O(67) δdCD$_3$C(10) [δsCD$_3$C(11)
1050	1042 *a*″	δdCD$_3$O(75) δdCD$_3$C(16)	1042	δdCD$_3$O(96)
1021^d	1036 *a*′	δdCD$_3$C(33) δCD$_2$(30) δwCD$_2$(19)	1033	δwCD$_2$(32) δrCD$_2$(25) δCD$_2$(24)
			1009	δdCD$_3$C(55) δrCD$_2$(12) δsCD$_3$O(12)
991	982 *a*′	νOC′(49) δrCD$_3$C(14) δdCD$_3$C(12) δOC′C(10)		
978^d	968 *a*″	δrCD$_2$(32) δdCD$_3$C(24) δrCD$_3$C(11)		
960			975	νOC′(57) δdCD$_3$C(12) δrCD$_3$C(10)
918^c	929 *a*′	νOC′(16) νCO(11) δwCD$_2$(10)		
913	912 *a*″	πC=O(25) δdCD$_3$O(24) δtCD$_2$(19) δrCD$_3$C(15)	918	πC=O(22) δtCD$_2$(21) δrCD$_3$O(21) δrCD$_3$C(14) [δrCD$_3$O(14)
	897 *a*″	δtCD$_2$(62) δrCD$_3$O(15) πC=O(12)	911	δtCD$_2$(21) δrCD$_3$C(17) πC=O(14)

862	859 *a*′	νCO(17) δCCO(13) νC′C(13)	889	νC′C(18) δrCD$_3$C(16) δsCD$_3$C(13)
839		[δsCD$_3$C(11)		
816	816 *a*′	δrCD$_3$O(34) νC′C(12) δsCD$_3$C(11)	842	δrCD$_3$O(21) δCCO(17) δtCD$_2$(15)
784				[νCO(14)
725			779	νCO(23) δrCD$_3$O(22) δtCD$_2$(13)
717	715 *a*′	δrCD$_3$C(43) δwCD$_2$(22) νOC′(17)	732	δrCD$_3$C(27) νOC′(16) δwCD$_2$(15)
583	570 *a*′	δC=O(39) νCC(18) δrCD$_3$O(14)		[νCC′(11)
	603 *a*″	δrCD$_2$(52) δrCD$_3$C(51) [νOC′(13)	567	δC=O(33) δrCD$_2$(15) νCC(12)
572				[νOC′(11)
527			603	δrCD$_2$(38) δrCD$_3$C(42)
518^d	519 *a*″	πC=O(54) δrCD$_3$O(53)	528	πC=O(51) δrCD$_3$O(55)
408				
384	383 *a*′	δCCO(92) δrCD$_3$O(29) δC=O(18)	406	δCCO(35) δOC′C(32) δC=O(21)
		δOC′C(14)		[δCOC(21)
346	350 *a*′	δOC′C(37) δCOC(21) δC=O(12)		
274			341	δOC′C(42) δCCO(51) δrCD$_3$O(12)
	189 *a*″	τCD$_3$C(83) τCD$_3$O(10)	271	δCOC(37) δCCO(25) τCD$_3$C(15)
185	187 *a*′	δCOC(42) δOC′C(39) δCCO(22)		

Calculated wavenumbers higher than 2000 cm^{-1}: 2235 2226 2224 2212 2200 2122 2103 2078.

[a] See footnote [b] to Table 1 for abbreviations. [b,c,d] See footnotes to Table 3.

trum, suggesting the presence of two molecules, or an even number of molecules, in the crystal unit. This would also explain some commonly observed band splits. Additionally, on crystallization, some bands disappear because of the elimination of unstable conformers and new bands appear owing to the higher resolution at lower temperatures. Therefore, it is of importance to examine crystalline-state spectra, as well as liquid-state spectra.

In the Raman spectra of crystalline E-NCA-d_0 and -d_3 (top in Figs. 1 and 2), besides the νC=O bands, six characteristically strong bands appear near 1460, 1450, 1120, 850(885), 635(595), 380(370) cm^{-1}, the number in parentheses being the observed wavenumber of the corresponding band in E-NCA-d_3. In the spectra of crystalline E-NCA-d_5 and -d_8 (top in Figs. 3 and 4), three bands near 865(885), 625(585), 345 cm^{-1} (corresponding to the last three bands of E-NCA-d_0 and -d_3), and new bands near 1195, 965(985) and 725(715) cm^{-1} are prominent. The appearance of such strong bands at positions common to E-NCA-d_0 and -d_3, and E-NCA-d_5 and -d_8, indicates that the deuteration of the ethyl group has a greater influence on Raman intensity than deuteration of the acetoxy methyl group.

Thus, a clue as to how to assign these bands of E-NCAs is found in the results of a previous study on the Raman spectra of ethyl trichloroacetate and its deuterate (E-TCA-d_0 and -d_5), whose molecules in the crystalline state exist only in the *trans–trans–trans* conformer about CCl–CO–O–CH_2CH_3 axes [11].

A band assignment analogous to that for E-TCA-d_0 and -d_5, may be made for the six strong bands of E-NCA-d_0 aand -d_3, allocating them to the two $\delta d CH_3C$*, $\delta\nu CH_3C$, νC–C, δC=O and δOC′C modes, in descending wavenumber order, and similarly the three new bands of E-NCA-d_5 and -d_8 are assigned to $\delta w CD_2/\nu OC'$, $\delta r CD_3C/\delta t CD_2$ and $\delta r CD_3C$ modes. The weak Raman bands near 1483 and 1472, 1400, 1275, 1265, 1160, 940(910), 600(525) and 435(410) cm^{-1}, which are observed commonly in both E-NCA-d_0 and -d_3 spectra, correspond to the bands at 1475[δCH_2], 1398[$\delta s CH_3C$], 1303[$\delta t CH_2$], 1266[νC–O], 1146[$\delta r CH_3C$], 970[νC′–C], 684[πC=O] and 449 cm^{-1} [δCCO] for E-TCA-d_0 in the *trans* conformer. On the other hand, the Raman bands near 1095, 1055, 915, 605(515), 585 and 420(380) cm^{-1} observed in both the E-NCA-d_5 and -d_8 spectra are associated with the bands at 1090[$\delta s CD_3C$], 1052[$\delta d CD_3C$], 908[νC′–C], 683[πC=O], 589[$\delta r CD_2$] and 410 cm^{-1} [δCCO] of E-TCA-d_5, respectively.

More careful analysis to identify CH_3O* vibrations shows that the bands near 1425, 1376 and 1361(1370), 1004(966), and 942 cm^{-1}, present in the E-NCA-d_0 and -d_5 spectra but absent in the E-NCA-d_3 and -d_8 spectra, should be assigned to the $\delta d CH_3O$, $\delta s CH_3O$ and two $\delta r CH_3O$ modes, respectively. The deuteration of the acetoxy methyl group shifts them to lower frequencies; the

---

*A distinction between the two methyl groups of E-NCA is made by designating the methyl group of ethyl radical by CH_3C and the acetoxy methyl group by CH_3O.

δCD_3O bands are observed near 1080 and 1020 cm^{-1} and δrCD_3O bands at 790(816) cm^{-1}. The CH_3O vibrations correspond to the bands at 1446 and 1439, 1379, 1020, and 976(944) cm^{-1} of methyl- and trideuteromethyl-acetate (M-NCA-d_0 and -d_3) and the CD_3O vibrations to the bands at 1035 and 993, and 778(832) cm^{-1} of methyl trideuteroacetate and full deutero analogue (M-NCA-d_3' and -d_6) [19].

The IR spectra of E-NCAs exhibit some characteristic bands at positions corresponding to the Raman bands. Two strong and broad bands appear at 1241 and 1048 cm^{-1} in the liquid-state spectrum of E-NCA-d_0 and have been assigned to the νC–O and νO–C′ modes, respectively [13]. Almost certainly the former band shifts progressively to higher wavenumber with increasing deuteration. Moreover, on crystallization the νC–O band positions shift to higher wavenumber. The νO–C′ band is increasingly surrounded by CD_3 and CD_2 deformation bands with increasing deuteration and seems to lose its prominent nature. Also, the high intensity of the 1033 cm^{-1} band of E-NCA-d_5 suggests a vibrational nature similar to the 1048 cm^{-1} band of E-NCA-d_0. The band of E-NCA-d_8 at 916 cm^{-1} corresponds to the 923 cm^{-1} band of E-NCA-d_3. An extensive explanation of C–H(C–D) stretching vibrations is given by Nolin and Jones [13].

Vibrational coupling of skeletal stretching vibrations

The conventional description used above for band assignment is only approximate and if a more detailed assignment is necessary, the PED in Tables 3–6 should be consulted. The detailed expression indicates that vibrational coupling exists among a few vibrations. In particular, skeletal stretching vibrational coupling is quite strong. As mentioned above, the bands near 1260, 1050, 940 and 845 cm^{-1} of E-NCA-d_0 are assigned to the νCO, νO′C, νC′C and νCC modes, respectively. In addition to νCO contribution, the 1260 cm^{-1} band has νCC (large) and δC=O contributions, and the 1050 cm^{-1} band has νOC′ and νC′C contributions, while the 845 cm^{-1} band does not have the essential νCC but has a large νOC′ contribution. A similar picture of vibrational coupling was seen in E-TCA-d_0, though the band at 882 cm^{-1} had an essential νCC contribution.

The PED of the νCO band of E-NCA-d_0 is similar to those of the other three E-NCAs. In the other skeletal bands, the stretching vibration contribution is reduced with increasing deuteration, because of additional couplings with deformation vibrations of methyl and ethyl groups. It is difficult to make a clear-cut assignment.

Rotational isomerism and band pairs of trans/(gauche) *conformers*

An important clue in the problem of rotational isomerism would be the discovery of band pairs coming from a single mode, in the liquid-state spectra, one component of which disappears on crystallization. Such band pairs seem to exist in the liquid-state spectra of E-NCAs, as they do in the liquid-state spectra of E-TCAs, where they are associated with the *trans*/(*gauche*) conformers of the CO–CH_2CH_3 axis [11]. In Table 7 the band pairs of E-NCAs are summarized together with the observed and calculated wavenumbers, and band assignment.

We have discussed the problem of the band pairs of $XC(C{=}O)OCH_2CH_3$ type esters (X = H, Cl, N≡C–, CH_3–, N≡C–CH_2– and CCl_3–) previously [11]. In the present study we have also found many band pairs of the deuterates. The results of the normal coordinate calculation suggest that bands observed near 1300 cm^{-1} [$\delta t CH_2$] of the d_0 and d_3 compounds, the bands near 800 cm^{-1} [$\delta r CD_3O$] of the d_3 and d_8, and bands near 1200 [$\delta w CD_2/\nu OC'$] and 730 [$\delta r CD_3C$] cm^{-1} of the d_5 and d_8 esters, are band pair members, also.

All the esters previously discussed, and esters with X = CH_2Cl– and $CHCl_2$– [6, 7], show, in their liquid-state spectra, a band pair corresponding to the pair 1116/(1095) cm^{-1} of E-TCA-d_0 [$\delta r CH_3C$]. Since the E-TCA molecule (having a complete *Cs* symmetry [20]) exists as a conformer of all *trans* skeletal axes in the crystalline state [11], the presence of such a band pair in the liquid-

TABLE 7

Band pairs of *trans–trans* (*T*) and *trans–gauche* (*G*) conformers

E-NCA-d_0		E-NCA-d_3		E-NCA-d_5		E-NCA-d_8		Assignment	
ν_{obs}	ν_{cal}	ν_{obs}	ν_{cal}	ν_{obs}	ν_{cal}	ν_{obs}	ν_{cal}		
1301	1304	1302	1305					$\delta t CH_2$	(*G*)
1262	1265	1276	1278						(*T*)
1262	1265	1268	1265	1273	1277	1290	1277	νC–O	(*T*)
1241	1256	1259	1253	1267	1272	1280	1272	+νCC	(*G*)
				1197	1198	1196	1198	νC′C	(*T*)
				1182	1174	1178	1174	+$\delta w CD_2$	(*G*)
1114	1125	1116	1126	730	722	717	715	$\delta r CH_3C$	(*T*)
1099	1106	1098	1104	743	739	725	732		(*G*)
938	939	915	910					νC′C	(*T*)
918	911	897	887					+νOC′	(*G*)
814	815	811	812	590	584	583	603	$\delta r CH_2$	(*T*)
786	790		813	581	586	572	603	+$\delta r CH_3C$	(*G*)
		790	791			816	816	$\delta r CD_3O$	(*T*)
		760	769			784	779		(*G*)
608	616	531	532	611	613	527	528	πC=O	(*G*)
	609	523	522		625	518	519	+$\delta r CH_3O$	(*T*)
463	463	439	433	438	441	408	406	δCCO	(*G*)
441	441	409	400	423	428	384	383	+δOC′C	(*T*)
314	314	300	306	279	276	274	271	δCOC	(*G*)
209	209	200	201	200	194	185	187	+δCCO	(*T*)

state spectra of ethyl esters is an important indication of a *trans–gauche* isomerism coming from ethyl groups.

Strangely, in contrast to other ethyl chloroacetates [11, 21], the δOC′C vibration of E-NCAs does not appear as a band pair probably because of the absence of heavy α-substituents.

There are some bands whose positions change considerably on the change of state. E-NCA-d_0 gives a strong IR band at 1241 cm^{-1} in the liquid and at 1261 cm^{-1} in the crystalline state. It is probable that the 1241 cm^{-1} band is also a band pair with two components which are apparently unresolvable owing to their very broad and strong absorptions.

Bands in the region below 700 cm^{-1}

Besides the $\delta r CD_2$ band (ca. 590 cm^{-1}) of E-NCA-d_5 and -d_8, each E-NCA is expected to give nine fundamental bands in the region below 700 cm^{-1}; the five deformations: δC=O, πC=O, δCCO, δCOC, δOC′C and the four torsions: τCH_3O, τC–O, τO–C′, τCH_3C. In crystalline-state spectra, seven fundamental bands are clearly detected, as summarized in Table 8. Surprisingly, the 284 cm^{-1} band of E-NCA-d_0 seems to be absent in the liquid-state spectra. In contrast, the 314 cm^{-1} band of liquid E-NCA-d_0, distinguished from crystalline bands by parentheses in Table 8, disappears on crystallization. At first sight, both the bands for E-NCA-d_0 (-d_3) look like the two components of a band pair, but the large separation in wavenumber between the corresponding bands for E-NCA-d_5 (-d_8) casts doubt on this hypothesis. The 284 cm^{-1} band seems to be due to a shift to higher wavenumber, on crystallization, of a very weak band observed at 254 cm^{-1} in the liquid-state IR spectrum.

Let us now consider the observed wavenumbers for the vibrations displayed

TABLE 8

Observed wavenumbers for crystalline E-NCAs in the region below 700 cm^{-1} and wavenumber differences between E-NCAs

E-NCA-d_0	-d_3	-d_5	-d_8	d_0-d_3	d_5-d_8	d_0-d_5	d_3-d_8	Assignment
635	595	623	583	40	40	12	12	δC=O
603	523	608	518	80	80	−5	5	πC=O
438	410	419	382	28	37	19	28	δCCO
380	370	347	344	10	3	33	26	δOC′C
(314)	(298)	(279)	(271)	(16)	(8)	(35)	(27)	δCOC (*G*)
284	282	222	221	2	1	62	61	$\tau CH_3(CD_3)C$
211	203	197	190	8	7	14	13	δCOC (*T*)
151	148	150	148	3	2	1	0	τC–O

The wavenumber is the stronger of IR or Raman bands, or the average value if their intensities are similar.

in Table 8. The value of d_0-d_3 or d_5-d_8 for a vibration is the variation in wavenumber on deuteration of the acetoxy methyl group, and d_0-d_5 or d_3-d_8 is that of the ethyl group. From these variations it can be deduced which of the two groups or their related modes contributes more to each vibration. From this standpoint, the bands at 635, 603, and probably 438 cm^{-1}, of E-NCA-d_0 are associated with the δC=O, πC=O and δCCO modes due to the acetoxy methyl rather than the ethyl group, while the bands at 380, (314) and 284 cm^{-1} are associated with the δOC′C, δCOC(G) and τCH_3C modes due to the ethyl group, respectively.

The assignment of the 635, 603, 438 and 380 cm^{-1} bands is highly satisfactory, and consistent with that made by analogy with the spectra of E-TCAs. It is also supported by the results of the normal coordinate calculation and Ogawa's study of E-NCA-d_0 [14]. The wavenumber ratio $\nu(d_0)/\nu(d_5)$ or $\nu(d_3)/\nu(d_8)$ of the τCH_3C band to the τCD_3C band is in both cases 1:28, confirming the validity of the assignment. This assignment is also supported by the fact that the three τCH_3C (τCD_3C) contributions of *tert*-butyl formate concentrate the bands near 263(209) cm^{-1} [22], and that the bands of other ethyl compounds appear near 270(205) cm^{-1} [23].

It should be noted that the δOC′C band is characteristically strong in Raman spectra, since this band corresponds to one member of the k_1 array (the so-called LAM-1 accordion-like motion) in the $\nu_5(\delta CCC)$ mode [24] for $CH_3COO(CH_2)_nCH_3$.

The band corresponding to the (314 cm^{-1}) band of E-NCA-d_0 appears at almost the same position in the liquid-state spectra of ethyl chloroacetates and also disappears on crystallization [11, 21], or becomes weak at low temperature (dichloro-derivative) [21]. On the other hand, methyl analogues, M-NCA and their α-chloro-derivatives, give the δCOC band at much the same position in both the liquid- and crystalline-state spectra [8–10, 14, 19, 25, 26].

All the torsions, except that of τCO, are expected to change their positions on deuteration of acetoxy methyl or ethyl groups, as does the τCH_3C band at 284 cm^{-1} of E-NCA-d_0. When the ethyl group is deuterated the 211 cm^{-1} band shows very little change ($\nu d_0/\nu d_5 \doteqdot \nu d_3/\nu d_8 = 1.07$), as does the 151 cm^{-1} band. The τC–O modes of ethyl chloro- and cyano-formates were associated with bands at 148 and 143 cm^{-1}, respectively [27]. Accordingly, the 151 cm^{-1} band is assigned to the τC–O mode of E-NCAs. On the other hand, since the 211 cm^{-1} band cannot be considered to arise from the τCH_3–O and τO–CH_2 modes, we assign this band to the δCOC mode in the *trans* conformer with the aid of the normal coordinate calculation.

ACKNOWLEDGEMENTS

One of us (Y. M.) wishes to express his sincere thanks to Comisión Asesora de Investigación Científica y Técnica (Ministerio de Educación y Ciencia, Spain), which provided financial support for scientific research at the Universidad Complutense de Madrid. The authors also wish to thank Mr. Naoki Kakizawa of Kobe University for his experimental assistance, and the Information Processing Center of Hiroshima and Kobe University for the use of a HITAC M-680H and a NEAC ACOS 1000 system, respectively.

REFERENCES

1 L. J. Bellamy, The Infrared Spectra of Complex Molecules, Vol. 1, 3rd edn., Chapman and Hall, London, 1975, Chap. 11.
2 G. I. L. Jones and N. L. Owen, J. Mol. Struct., 18 (1973) 1.
3 S. W. Charles, G. I. L. Jones and N. L. Owen, J. Chem. Soc. Faraday Trans. 2, 69 (1973) 1454.
4 M. G. Dahlqvist, Spectrochim. Acta, Part A, 36 (1980) 37.
5 A. Hernanz, M. V. García and J. Morcillo, J. Mol. Struct., 80 (1982) 335.
6 M. A. Raso, M. V. García and J. Morcillo, J. Mol. Struct., 115 (1984) 449.
7 M. A. Raso, M. V. García and J. Morcillo, J. Mol. Struct., 142 (1986) 41.
8 Y. Mido and M. Hashimoto, J. Mol. Struct., 129 (1985) 253.
9 Y. Mido and M. Hashimoto, J. Mol. Struct., 131 (1985) 71.
10 Y. Mido, K. Suzuki, N. Komatsu and M. Hashimoto, J. Mol. Struct., 144 (1986) 329.
11 Y. Mido, T. Kawashita, K. Suzuki, J. Morcillo and M. V. García, J. Mol. Struct., 162 (1987) 169.
12 Y. Mido, N. Komatsu, J. Morcillo and M. V. García, J. Mol. Struct., 172 (1988) 49.
13 B. Nolin and R. N. Jones, Can. J. Chem., 34 (1956) 1392.
14 Y. Ogawa, Ph. D. Thesis, The University of Tokyo, Tokyo, 1978.
15 Structure Data of Free Polyatomic Molecules, Landolt-Börnstein, Numerical Data and Functional Relationships in Science and Technology, New Series, Group II: Atomic and Molecular Physics, Vol. 7, Springer-Verlag, Berlin, 1976.
16 T. Shimanouchi, H. Matsuura, Y. Ogawa and I. Harada, J. Phys. Chem. Ref. Data, 7 (1978) 1323.
17 H. Matsuura and M. Tasumi, in J. R. Durig (Ed.), Force Fields for Large Molecules, Vibrational Spectra and Structure, Vol. 12, Elsevier, Amsterdam, 1983, Chap. 2, pp. 69-143.
18 Definition and Symbolism of Molecular Force Constants, IUPAC Commission on Molecular Structure and Spectroscopy, Pure Appl. Chem., 50 (1978) 1707.
19 W. O. George, T. E. Houston and W. C. Harris, Spectrochim. Acta, Part A, 30 (1974) 1035.
20 M. Hashimoto, M. Watanabe and H. Takada, J. Magn. Reson., 34 (1979) 553.
21 Y. Mido, M. A. Raso, M. V. García and J. Morcillo, unpublished data.
22 Y. Omura J. Corset and R. M. Moravie, J. Mol. Struct., 52 (1979) 175.
23 J. R. Durig and H. L. Heusel, J. F. Sullivan and S. Cradock, Spectrochim. Acta, Part A, 40 (1984) 739.
24 R. F. Schaufele, J. Chem. Phys., 49 (1968) 4168.
25 J. E. Katon and D. Sinha, Spectrochim. Acta, Part A, 33 (1977) 45.
26 R. Fausto and J. J. C. Teixeira-Dias, J. Mol. Struct., 144 (1986) 225; 241.
27 S. W. Charles, G. I. L. Jones, N. L. Owen, S. J. Cyvin and B. N. Cyvin, J. Mol. Struct., 16 (1973) 225.